INCREASING THE DAMPING PROPERTIES OF CARBON LAMINATES BY FLAX FIBER HYBRIDIZATION FOR ROTORCRAFT APPLICATIONS

Jonas John * Lukas Gaugelhofer † Manfred Hajek ‡

Institute of Helicopter Technology
Technical University of Munich, 80333 Munich, Germany

Vibrations play a crucial role in the design of helicopter structures and are in many cases the cause for structural changes in the late development phase. Often, dynamic interactions and excitations can only be determined in flight tests while structural dynamic simulations can only make inaccurate predictions. This is even more true for unconventional designs such as eVTOLS, for which practical experience is limited. One possible solution to minimize risks in the design is to increase the global damping in the helicopter structure, for which natural fibers offer a promising approach. This paper lays the groundwork for further investigations using flax fibers in hybridization with carbon fibers for selective damping enhancement of helicopter structures. For this purpose, the damping of flax, carbon and flax/carbon hybrid laminates is investigated at laminate level. High-performing flax and carbon prepregs were used to manufacture test specimen in a vacuum/autoclave process. Experimental modal analyses, using a contactless measurement method and impulse technique, were performed on hybrid and non-hybrid laminate test specimen with different stacking sequences and flax contents to determine their dynamic behavior. The damping is calculated using the Half-Power Bandwidth Method and set in relation to their mechanical properties, quantifying the damping potential for different load cases. The superior damping potential of flax was confirmed, especially in fiber direction. The distance to the neutral axis was shown to be the main influence between the oppositely behaving stiffness and damping in the laminates. However, the use of flax fibers in the hybrid laminates made it possible to achieve an advantageous ratio in favor of the damping. Flax fiber orientation in the direction of loading (UD0) is particularly suitable for this purpose.

NOMENCLATURE

E	Young's modulus
E^I, E^{II}	Primary & secondary bilinear Young's modulus
H	Hybridisation based on flax fiber content
f	Frequency
f_n	Eigenfrequency
l	Coupon free beam length
t	Beam thickness in vibration direction
η	Loss factor
ρ	Density
UD	Unidirectional fabric
FRF	Frequency Response Function
HPB	Half-Power Bandwidth Method

* Graduate Research Assistant, jonas.john@tum.de
† Graduate Research Assistant, lukas.gaugelhofer@tum.de
‡ Professor and Department Head, hajek@tum.de

Presented at the 48th European Rotorcraft Forum, Winterthur, Switzerland, 6-8 September, 2022.

1. INTRODUCTION

Vibrations are a constant challenge in helicopter development and a frequent cause of delays in development time [2]. According to Datta [2], numerous components of the helicopter are involved in vibration generation and propagation. With the main rotor as the primary source, other sources can also be found in the helicopter system dynamics which include the tail rotor, engines, and the gear box. Apart from mechanical sources, there are further aerodynamic causes, particularly the rotor and cell wake interactions with the tail boom or empennage. Aerodynamic interference by the rotor and fuselage wake and the tail boom and empennage causes vibrations, especially at low speeds and fast forward flight [2]. The components mentioned above influence each other and are strongly coupled. For example, main rotor vibrations are mechanically transmitted to the airframe, and airframe vibrations, in turn, excite the rotor dynamics [2]. The so-called "tail-shake" phenomenon or "Flutter" are some of the possible consequences [3, 4]. This high level of vibrations often requires additional vibration reduction measures in the form of isolation systems [5] and vibration absorbers [6]. Interactions

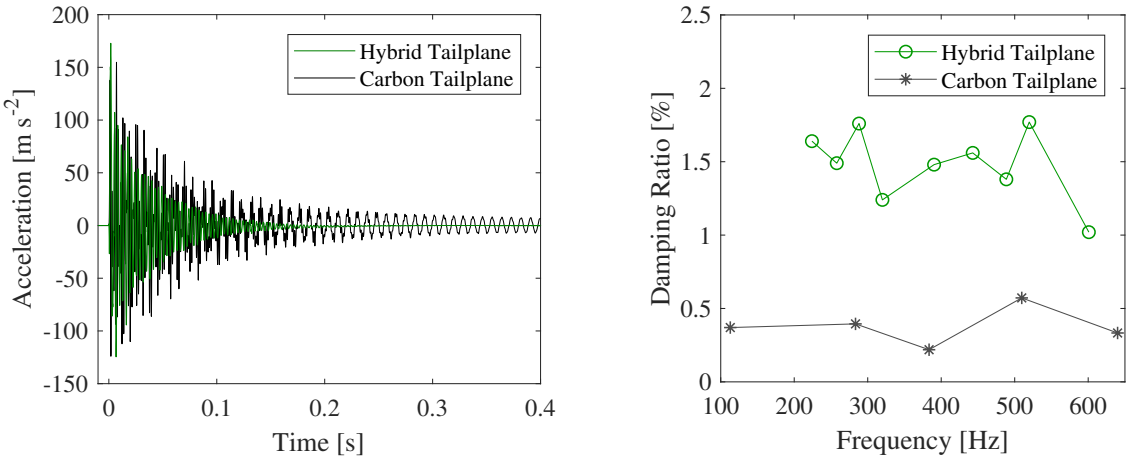

Fig. 1: Accelerations over time (left) and damping ratio over frequency (right) compared for a carbon and a flax-carbon hybrid helicopter tail plane [1]

of the blade tip vortices and the rotor wake can lead to vibrations of the tail units [7, 8], which have to be reduced by unique tuning or dynamic isolation of the fuselage structure and the tail [8]. Often, a re-design is necessary during the flight test phase, resulting in high costs and delays in development times [9, 10]. In order to control these vibration mechanisms, the structure must be damped as much as possible to keep load amplitudes and the general vibration level of the cabin low. Possible solutions are using elastomer layer damper concepts comparable to the rotor blade damping [11]. Other approaches in composite design discuss adding visco-elastic materials into the laminate [12]. A further alternative proposed in this work is to increase the damping of the fiber composite structure of the tailplane/tail boom by using natural fibers. These exhibit high inherent damping and can thus contribute to the damping of the overall component using a hybrid flax-/carbon design [13]. This results in the advantage that no non-load bearing mass is added and the damping can be increased not only locally for single mode shapes but integrated into the whole structure. Thus, this variant offers a unique potential for future helicopter and aeronautical structures.

Flax fibers have long since gained a foothold as structural materials in other industries, such as the automotive industry, e.g., in complex and high-quality door structures in the mid-range and luxury classes [14]. Nevertheless, they are still at the research stage in aerospace applications. In the area of stiffness and failure criteria of flax materials, significant progress has been made recently, as it has been shown that competitive helicopter components like tail units can be designed [1, 13]. However, the prediction and optimization of the damping properties, especially when integrated in Carbon Fiber Reinforced Plastics (CFRP), is still largely unresolved. For example, Henschel [1] was able to determine higher damping during the production of a flax-carbon hybrid tailplane compared to a reference carbon tailplane. As shown in Fig.1 significantly faster decay of the accelerations and higher damping ratios were observed for the hybrid tailplane investigated at the Technical University of Munich. The damping ratio was more then three times higher. However, her design and investigations did not have damping as an optimization goal, but rather structural stiffness and a high organic content. The influence of flax hybrid design specifically on the damping behavior was not yet part of the study. By investigating the influencing factors in the design, it is possible that the damping can be even further improved. Therefore, for a target-oriented use of flax fibers in aerospace structures specifically for damping enhancement, it is necessary to gather further knowledge and predictive capabilities about the damping properties of flax-carbon hybrids.

While there have been previous studies about damping properties of flax and flax-carbon hybrid composites like in Ameur [15], Duc [16], Fairlie [17] or Assarer [18, 19], this study focuses not only on the investigation of unidirectional fiber composites but also on the promising combination of different fiber orientations in the hybridization. Furthermore, using a high-performing prepreg system improved the mechanical properties and fiber volume fraction of the flax laminate significantly when compared to vacuum infusion or hand-laminating processes, limiting the transferability of the results. Therefore, this paper presents new experimental data about the damping properties of flax and flax-carbon hybrid composite laminates over a wide range of fiber orientations, stacking sequences, and their relations regarding the mechanical properties. This provides the basis for developing a detailed material model for damping simulation and understanding the application in more complex aerospace structures such as spars and wing profiles up to complete tail structures.

2. MATERIAL AND PRODUCTION

For the proposed investigation, various flax materials from different manufacturers on the market were considered. As shown in another study of this institute by Gaugel-

hofer [20], the offered flax products differ strongly in their mechanical properties. This applies not only to the different fibers but also to the resins and the manufacturing process used. Prepreg systems perform particularly well and can score with higher fiber volume contents and therefore better mechanical properties. In addition, they are easier to manufacture and more convenient to lay. Due to the good mechanical properties [20], the existence of twill and unidirectional (UD) material, and the availability of a carbon prepreg with the same resin system, the manufacturer FIBERPREG was chosen for the present investigations. The BCOMP flax fibers used in this prepreg exhibited above-average damping values compared to others in the damping investigations of Duc [21], who used a different manufacturing process (vacuum infusion) and resin. The materials used and their Tensile moduli are listed in Table 1. Due to the bilinear behavior of flax, the table lists two values for the Tensile Moduli (E^I and E^{II}). The values for carbon are taken from FIBERPREG's datasheets, while the flax laminates were determined experimentally.

FIBERPREG PrePreg	E^I (in *GPA*)	E^{II} (in *GPA*)
Carbon C150 UD EP4.5 33	135*	-
Carbon C200 Twill 3K EP4.2	71*	-
Flax NAT-150 UD EP1.5	25.08**	17.61**
Flax NAT-200 Twill EP1.5	12.27**	08.84**

** from datasheet ** from tensile test [20]*

Table 1: Material designations and the associated Tensile modulus E1 and E2 for bilinear material behavior

The laminate test coupons were manufactured using a prepreg autoclave process. The patches were manually layed on a steel plate in 30cm x 30cm dimensions and packed in vacuum bags with -0.9 bar. The curing cycle was set according to manufacturer specifications 120°C for 90 min at 5 bar. The heating rate was set to 2 min/°C. This achieved fiber volume contents of over 50% in the flax plies, setting the study apart from previous damping studies. For example, Ameur [15] only achieved a flax content of 32%, using a hand laminating process. Since resins have a great influence on the viscous damping, it can be assumed that the damping properties change quantitatively.

3. METHODOLOGY

3.1 Laminates

Both non-hybrid and hybrid flax, carbon and flax/carbon composites were fabricated to determine their damping properties. A total of 24 different layups, 7 pure flax, 7 pure carbon and 10 hybrid laminates with different degrees of hybridization were examined. First, the fiber orientations as well as the sequence of the plies were investigated. The detailed ply design is summarized in Tbl.2. For a generic determination, different ply orientations and combinations were produced. In addition to the load cases 0°, 90° and 45°-135°, the influence of the distance of the edge layers to the neutral axis was also investigated by exchanging the fiber orientation inside and outside. For hybrids, only application-related load cases were investigated. For example, 90° carbon layers were not used, since they are not expected to make a significant contribution to either stiffness or damping. Attention was always paid to a symmetrical layup (as far as possible) in order to prevent bending-torsion coupling in the test. Two identical specimens were cut from each laminate in the form of bending bars with length 250 mm and width 25 mm. The thickness results from the number of plies and hybridization. Through the dimensions and weight of the manufactured coupon samples, the density was determined. Both the thickness t and the density ρ are listed in the Table 2.

3.2 Experimental Setup

A flexural vibration test was performed to determine the damping behavior of the laminate structures. The coupon specimens were tested in a free-clamped boundary configuration following ASTM E 756-98 [22, 23] . The test setup is shown in Fig.2. The pulse was excited with an automatic pulse hammer to generate the most reproducible results. The velocities of the free end of the beam were measured with a laser vibrometer. Signal analysis and processing was performed with Simcenter Testlab.

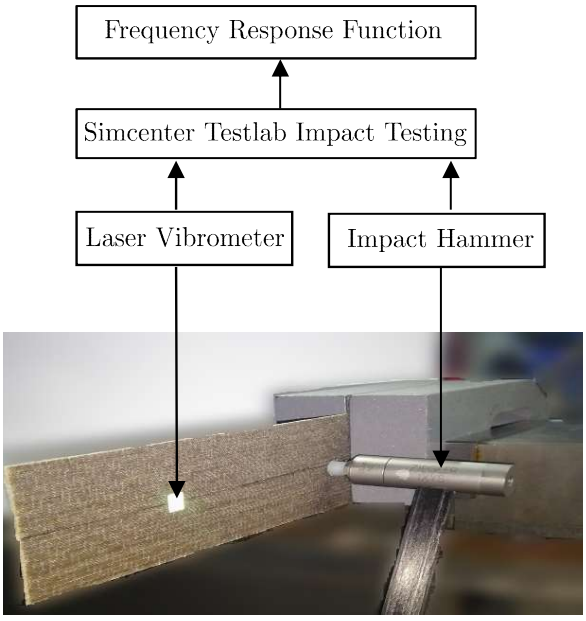

Fig. 2: Experimental setup of the Experimental Modal Analysis to determine the Frequency Response Functions

The exact dimensions of the experimental setup are shown in Fig.3. All specimens were measured in different lengths of the free end (l = 200, 190, 170, 150 and 130mm).

Laminates	Layup F = Flax UD, C = Carbon UD, FT = Flax Twill, CT = Carbon Twill	Hybridisation (H) (based on fiber weight flax)	Thickness t $[mm]$	Density ρ $[g/cm^3]$
Flax (Non Hybrid)				
$[F_3^0]_s$	F^0 / F^0 / F^0 / F^0 / F^0 / F^0	100%	1.25	1.16
$[F_3^{90}]_s$	F^{90} / F^{90} / F^{90} / F^{90} / F^{90} / F^{90}	100%	1.25	1.16
$[F_3^{45}]_s$	F^{45} / F^{135} / F^{45} / F^{135} / F^{45} / F^{135}	100%	1.25	1.16
$[F^0/F^0/F^{90}]_s$	F^0 / F^0 / F^90 / F^90 / F^0 / F^0	100%	1.20	1.16
$[F^90/F^90/F^0]_s$	F^{90} / F^{90} / F^0 / F^0 / F^{90} / F^{90}	100%	1.25	1.16
$[FT_3^{0-90}]_s$	FT^0 / FT^0 / FT^0 / FT^0 / FT^0 / FT^0	100%	1.65	1.16
$[FT_3^{45}]_s$	FT^45 / FT^{45} / FT^{45} / FT^{45} / FT^{45} / FT^{45}	100%	1.65	1.16
Carbon (Non Hybrid)				
$[C_3^0]_s$	C^0 / C^0 / C^0 / C^0/C^0 / C^0	0%	0.87	1.33
$[C_3^{90}]_s$	C^{90} / C^{90} / C^{90} / C^{90} / C^{90} / C^{90}	0%	0.87	1.33
$[C_3^{45}]_s$	C^{45} / C^{135} / C^{45} / C^{135} / C^{45} / C^{135}	0%	0.87	1.33
$[C^0/C^0/C^{90}]_s$	C^0 / C^0 / C^{90} / C^{90} / C^0 / C^0	0%	0.87	1.33
$[C^{90}/C^{90}/C^0]_s$	C^{90} / C^{90} / C^0 / C^0 / C^{90} / C^{90}	0%	0.87	1.33
$[CT_3^{0-90}]_s$	CT^0 / CT^0 / CT^0 / CT^0 / CT^0 / CT^0	0%	1.35	1.33
$[CT_3^{45}]_s$	CT^{45} / CT^{45} / CT^{45} / CT^{45} / CT^{45} / CT^{45}	0%	1.35	1.33
Hybrid				
$[C^0/F^0/C^0]_s$	C^0 / F^0 / C^0 / C^0 / F^0 / C^0	33%	1.01	1.25
$[F^0/C^0/F^0]_s$	F^0 / C^0 / F^0 / F^0 / C^0 / F^0	66%	1.13	1.20
$[F^0/C^0/C^0]_s$	F^0 / C^0 / C^0 / C^0 / C^0 / F^0	33%	1.01	1.26
$[C^0/C^0/F^0]_s$	C^0 / C^0 / F^0 / F^0 / C^0 / C^0	33%	1.01	1.23
$[F^{90}/F^{90}/C^0]_s$	F^{90} / F^{90} / C^0 / C^0 / F^{90} / F^{90}	66%	1.13	1.19
$[C^{90}/F^{90}/F^{90}]_s$	C^0 / F^{90}/ F^{90} / F^{90} / F^{90}/ C^0	66%	1.13	1.19
$[C^0/F^{90}/C^0]_s$	C^0 / F^{90} / C^0 / C^0 / F^{90} / C^0	33%	1.01	1.24
$[F_2^{45}/C^0/F^{45}]_s$	F^{45} / F^{135} / C^0 / F^{135} / F^{45} / C^0 / F^{135} / F^{45}	75%	1.55	1.23
$[C^0/F_3^{45}]_s$	C^0 / F^{45} / F^{135} / F^{135} / F^{45} / F^{135} / F^{45} / C^0	75%	1.55	1.21
$[F_2^{45}/C_2^0]_s$	F^{45} / F^{135} / C^0 / C^0 / C^0 / C^0 / F^{135} / F^{45}	50%	1.43	1.26

Table 2: Investigated Laminate Combinations and their degree of hybridization

	Coupon 1		Coupon 2	
Length (l) in mm	m_1 23,5 mm	m_2 140 mm	m_1 23,5 mm	m_2 140 mm
200	X	X	-	-
190	X	X	X	X
170	X	X	X	X
150	X	X	X	X
130	X	-	X	-

Table 3: Measurement configurations for each layup

The distance of the excitation point d from the clamping was constant at 12.5mm. The velocities were measured with the laser vibrometer at two different distances m_1 = 23.5mm and m_2 = 140mm.

With a free beam length of l=130mm, measurements were only taken at measuring point m1. For the second coupon per laminate, the length l=200mm was omitted. The different measurement variations are summarized in Table 3. This results in 16 different measurement configurations per ply structure and a total of 384 measurements. Due to the different measurement configurations, significantly more natural frequencies could be determined for one layup.

3.3 Measurement Evaluation

The frequency response functions (FRF) were determined from the measured velocity and force signals from the impact sensor using the SimLab software via the Fourier transformation. Fig.4 shows two examples of FRFs, one for a flax $[F_3^{45}]_s$ and a carbon $[C_3^{45}]_s$ specimen from the measurements up to 3000 Hz. The FRF can be used to determine the natural frequencies and thus the loss factor η_i through the Half-Power Bandwidth Method (HPB), where f_n is the natural frequency and f_1 and f_2 are determined as shown in Fig.5 [22].

$$\eta_i = \frac{\Delta f_n}{f_n} = \frac{f_2 - f_1}{f_n} \tag{1}$$

Fig.4 shows that the natural frequencies from carbon to flax are clearly more acute.

Furthermore, using ASTM E756 [22], the Young's moduli of the uniform beam specimens are determined with,

$$E_i = \frac{(12\rho l^4 f_n^2)}{(t^2 C_n^2)} \tag{2}$$

where ρ is the density of the beam, l the free beam length, t the thickness of the beam in vibration direction.

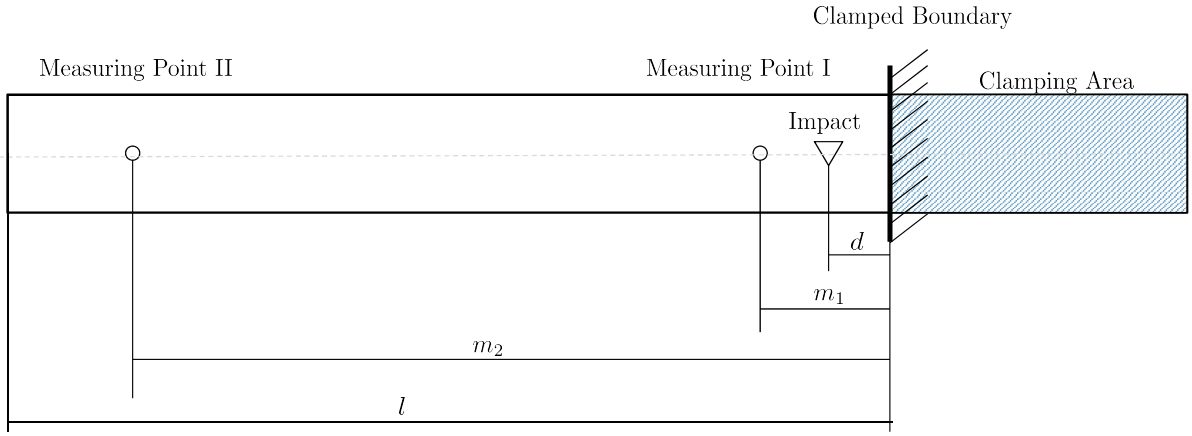

Fig. 3: Dimensions of the experimental setup

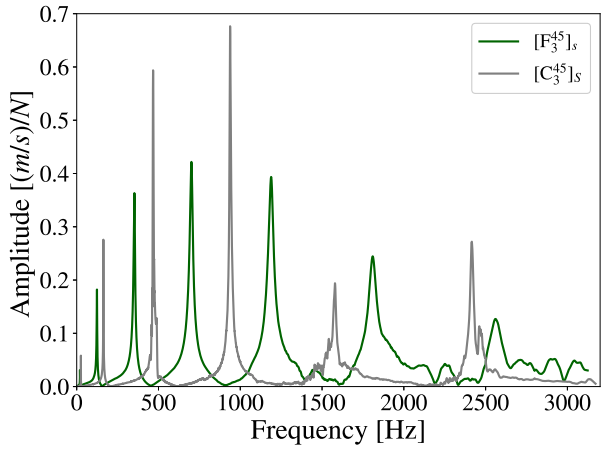

Fig. 4: Frequency Response Function of flax coupon $[F_3^{45}]_s$ and carbon coupon $[C_2^{45}]_3$ at m_1

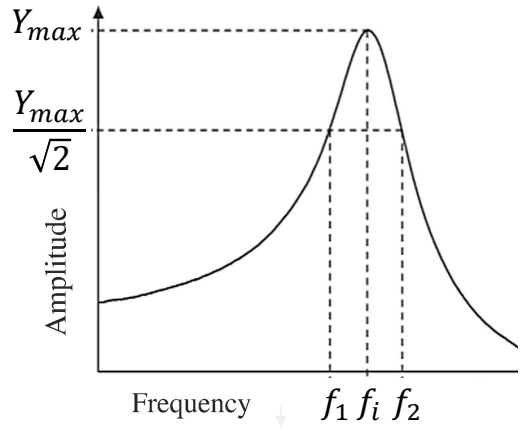

Fig. 5: Visualization of Half-Power Bandwidth Method

C_n is a mode n dependent coefficient for a clamped-free (uniform) beam. It is given in [22] as:

C_1= 0.55959,
C_2=3.5069,
C_3=9.8194,
C_4=19.242,2
C_5= 31.809,
C_n= $(\pi/2)(n-0.5)^2$, for $n > 3$

For each measurement, the natural frequencies and associated damping coefficients η_i and Young's modulus E_i were determined up to 3000 Hz. Due to the different clamping lengths, values could be determined over a wide set of frequencies. Nevertheless, because of the very light beams, it was not always possible to get enough energy into the system for each layup and measurement configuration to determine clearly defined natural frequencies over 1000 Hz. For this reason, the density of the determined natural frequencies decreases for higher frequencies.

3.4 Damping and Stiffness Analysis

For each layup, the modal loss factor and Yong's modulus show significant scatter for the investigated frequency range. Fig.6 shows all modal loss factor scatter points for an exemplary layup ($[F_2^{45}/C_2^0]_s$). The different measurement setups are represented by colors and markers. Each measured sample length is assigned its own color. In addition, a distinction by size is made between the two measurement points m_1 and m_2. Coupon 1 and Coupon 2 are each assigned a different symbol. A quasi-linear behavior over the frequency of the scatter could be determined for all layups and for both, damping and stiffness . Nevertheless, there was scatter and outliers, which increased with higher frequencies. Also, the first mode often demonstrated significantly higher loss factors. This effect was to be expected and is related to the fixed restraint. Due to friction in the restraint, the first eigenmodes are damped more

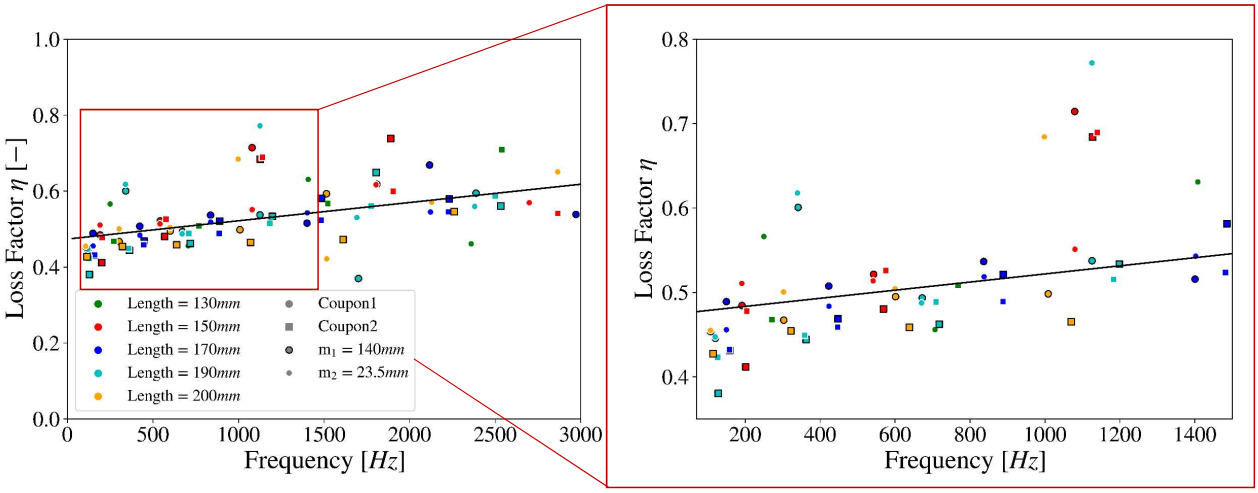

Fig. 6: Analysis of the scatter of modal damping values for the laminate $[F_2^{45}/C_2^0]_s$

intensively and thus cannot be assigned to material damping [15, 22]. For the creation of the damping models, the first modes were usually omitted in case a strong super elevation occurred as it can be seen in Fig.7. Looking at the measurements of the different coupons in Fig.6, it can be seen that, with a few exceptions, the damping values of one length are very close to each other. This is especially true for the range up to 1400 Hz. Here, the individual modes of the different lengths can be easily recognized as clusters of markers of the same color. This indicates a good reproducibility of the measurements in this range.

Strong outliers can occur for various reasons. In higher frequency ranges, the excitation of the mode certainly plays a role. Especially with very light composite samples and decreasing stiffness, it is difficult to excite the higher modes sufficiently. Furthermore, it cannot be excluded that torsional modes are also excited by asymmetries in the specimen or imperfect impacts. This can lead to superpositions with some bending modes and exaggerate the damping at certain points.

Overall, the results show a higher scatter with flax. This was also to be expected with flax as a natural material, since it has no continuous fibers and the fibers have a higher variation of material properties due to being natural. Accordingly, this is also to be expected for the damping properties and the stiffness. However, fluctuations in the measurement of the stiffness are significantly lower than for the damping.

The modal values obtained by the procedure described above can now be used to describe frequency-dependent damping and stiffness models. A first order least-square curve fitting approach allows the frequency-dependent damping model of each ply structure to be estimated as a linear as seen in Fig.7 for the Laminates $[F_3^0]_s$ and $[C_3^0]_s$. The loss factor $\eta(f)$ and Young's modulus $E(f)$ is thus mapped with a linear model in the form:

$$\eta(f) = A_\eta f + C_\eta \tag{3}$$

$$E(f) = A_E f + C_E \tag{4}$$

In order to keep the influence of outliers low, all points deviating more than 50% from the average value of all measurements were not taken into account for the use of the least-square method. In Fig.7 these points are marked with a red cross. Furthermore, in order to avoid that ranges with a particularly large number of measured points are evaluated disproportionately, clusters were combined in 30 Hz steps and a median was formed from this. These medians, shown as black dots, were then used to determine the linear models. The identical method was used for the Young's moduli. An evaluation of the individual laminates is presented in the following chapter.

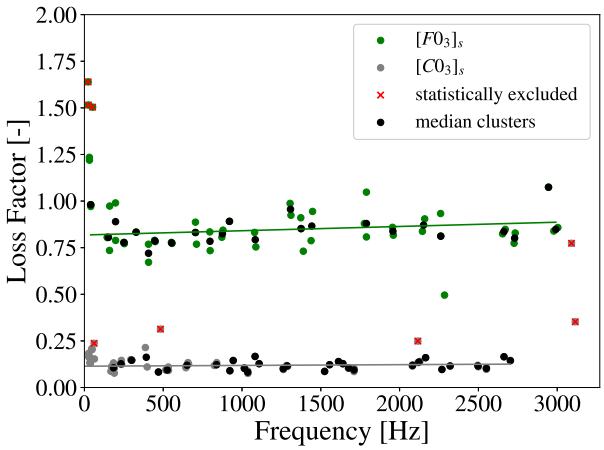

Fig. 7: Modal loss factor over frequency for two different layups $[F_3^0]_s$ and $[C_3^0]_s$

4. RESULTS AND DISCUSSION

4.1 Damping Evaluation

The results of the damping models for all laminates are shown in Table 4. In addition to the two constants describing the linear, a reference damping value at 50 Hz is given, as well as the hybridization (H). Looking at the slope of the models, almost all of the linears have a slightly positive gradient. This behavior is already known from other studies [21] and can be attributed, among other things, to the viscous behavior of the resin. As an exception, the laminates dominated with UD90 ($[F_3^{90}]_s$, $[C^{90}/C^{90}/C^0]_s$, $[C_3^{90}]_s$) show, similar to the flax twill $\pm 45°$ ($[FT_3^{45}]_s$) and the unidirectional carbon in fiber direction $[C_3^0]_s$, a negative slope A_η. The latter two, however, have minimal gradient and are quasi constant. For the three UD90 dominated laminates with negative slope of the damping over the frequency, a slight bending of the beam vertical to the fiber direction was always detected with out load. This may have led to additional effects especially at higher eigenmodes. In addition, these structures were difficult to excite up to high frequencies due to their low stiffness. These two effects can accordingly lead to a falsification of the results.

Loss Factor $\eta = A_\eta * f + C_\eta$ @ $f = 50\ Hz \Rightarrow \eta_{50}$

Laminates	A_η x 10^{-5}	C_η	η_{50}	H
Flax (Non Hybrid)				
$[F_3^0]_s$	2.285	0.818	0.819	100%
$[F_3^{90}]_s$	-65.754	2.458	2.426	100%
$[F_3^{45}]_s$	1.44	1.290	1.291	100%
$[F^0/F^0/F^{90}]_s$	2.917	0.841	0,842	100%
$[F^{90}/F^{90}/F^0]_s$	-20.912	1.693	1.682	100%
$[FT^{0-90}{}_3]_s$	6.250	0.850	0.854	100%
$[FT_3^{45}]_s$	-0.453	1.062	1.062	100%
Carbon (Non Hybrid)				
$[C^0{}_3]_s$	0.048	0.115	0.115	0%
$[C_3^{90}]_s$	-5.567	0.576	0.573	0%
$[C_3^{45}]_s$	2.358	0.348	0.349	0%
$[C^0/C^0/C^{90}]_s$	20.145	0.132	0.142	0%
$[C^{90}/C^{90}/C^0]_s$	2.898	0.309	0.310	0%
$[CT_3^{0-90}]_s$	2.321	0.180	0.181	0%
$[CT_3^{45}]_s$	2.527	0.443	0.444	0%
Hybrid				
$[C^0/F^0/C^0]_s$	1.535	0.213	0.214	33%
$[F^0/C^0/F^0]_s$	4.094	0.423	0.425	66%
$[F^0/C^0/C^0]_s$	1.881	0.429	0.430	33%
$[C^0/C^0/F^0]_s$	2.136	0.167	0.168	33%
$[F^{90}/F^{90}/C^0]_s$	14.314	0.912	0.919	66%
$[C^0/F^{90}/F^{90}]_s$	2.287	0.221	0.222	66%
$[C^0/F^{90}/C^0]_s$	2.023	0.183	0.184	33%
$[F_2^{45}/C^0/F^{45}]_s$	5.949	0.522	0.525	75%
$[C^0/F_3^{45}]_s$	2.049	0.272	0.273	75%
$[F_2^{45}/C_2^0]_s$	3.925	0.484	0.486	50%

Table 4: Frequency-dependent damping models for investigated laminates

The loss factor at 50 Hz (η_{50}) was chosen for comparing the different laminates with each other. Fig.8 compares all loss factors of the different ply structures of pure flax and pure carbon side by side. The clearly stronger damping behavior of flax compared to carbon is evident, with pure UD0 plies exhibiting the most substantial difference. Here, the dampening capacity of flax is seven times higher than carbon. The highest damping values for both materials occur at UD90, where flax still outperforms carbon by about a factor of four. In relation, carbon performs better here, since the viscous damping of the resin system dominates in UD90 plies and the fiber plays a smaller role.

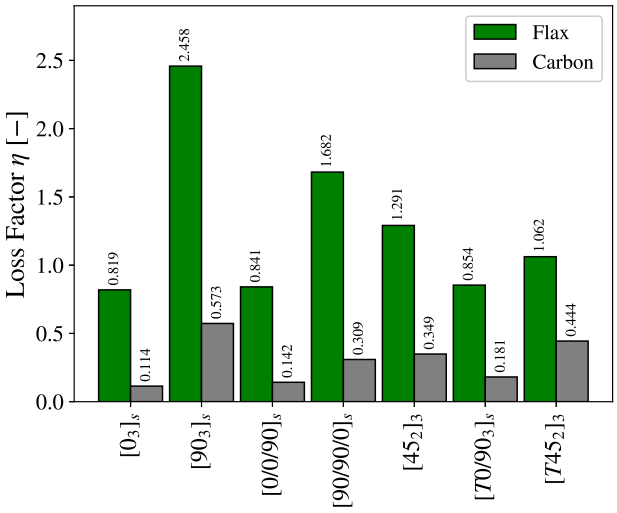

Fig. 8: Damping (loss factor) of flax vs. carbon with the same ply structure for $f = 50\ Hz$

With results at the specimens with multiaxial UD ($[0/0/90]_s$ and $[90/90/0]_s$), an effect already known from the literature is confirmed [15, 17]. Decisive for the damping values are the outer layers of the laminate, which are farthest away from the neutral axis. Central layers usually contribute only in small parts to the damping. Thus, despite the two UD90 plies in the interior, the laminate $[0/0/90]_s$ provides only marginally better damping than a pure UD0 specimen. Conversely, $[90/90/0]_s$ demonstrates a stronger damping potential which is closer to a pure UD90 specimen. However, the difference is greater here.

The damping of $[45_2]_3$ specimens is also increased compared to UD0. For carbon, it even exceeds the damping of $[90/90/0]_s$. For flax, $[45_2]_3$ also performs well and is 1.6 times higher than UD0.

The twill samples show another difference between carbon and flax. While the twill fabrics for carbon are significantly better damped than the comparable UD samples, especially at $[T45_2]_3$, this trend is not observed for flax. Thus, the damping in flax for woven fabrics $[T45_2]_3$ samples is even lower than for the comparable UD.

The loss factors η_{50} of the hybrid laminates are shown in Fig.9. The laminates are grouped according to their degree of hybridization and thus their flax content. The shading shows the dominant flax fiber orientation in the hybrid.

Again, it can be seen that the outer fibers dominate the damping behavior. Comparing, for example, $[C^0/C^0/F^0]_s$,

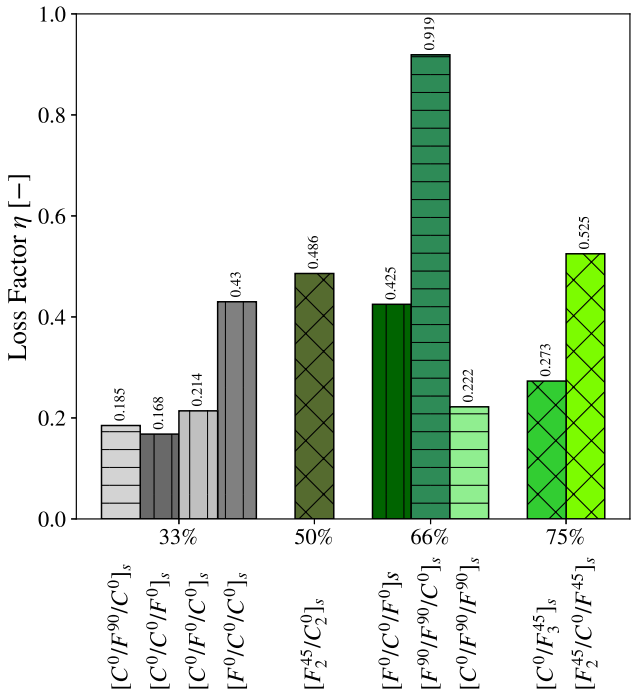

Fig. 9: Comparison of the damping values (loss factor) of hybrid laminates listed by degree of hybridization H (flax content in %) at $f = 50\ Hz$

$[C^0/F^0/C^0]_s$, and $[F^0/C^0/C^0]_s$, it can be deduced that the further the flax fiber is placed to the outside, the more the damping increases. Thus, even the two flax layers inside the laminate contribute to a doubling of the damping compared to pure carbon. If the flax layer is directly under the top layer, the damping increases by 60%. If the flax layer is the outer layer, the damping increases by 340% with a flax fiber content of 33%.

The laminate $[F^{90}/F^{90}/C^0]_s$ has the highest damping among the hybrids with 0.919. However, compared to the pure flax laminate with the same ply orientation ($\eta_{50} = 1.82$ $[F^{90}/F^{90}/F^0]_s$), the damping is significantly lower.

In general, the increase in damping due to UD90 in the hybrid is significantly less effective than with 100% flax content. Thus, despite the high flax and UD90 content, the $[C^0/F^{90}/F^{90}]_s$ laminate has only slightly higher damping than the $[C^0/F^0/C^0]_s$ laminate.

The influence of 45° plies is also significantly lower in the hybridization than in pure flat specimens. Nevertheless, the laminates with a 45/135° ply result in a significant increase in damping. A $[45_2]_3$ center ply contributes the least to the damping.

4.2 Stiffness Evaluation

The results of the stiffness models for all laminates are shown in Table 4. All 0° dominated laminates show a decrease in stiffness over frequency, while at 90° and 45° the stiffness increases. This is also true for all the hybrid laminates. The laminate $[C^0/C^0/C^{90}]_s$ is notable with a very high decreasing stiffness over frequency. In parallel, the slope of the damping over the frequency also shows a notably high decrease of stiffness. This is probably due to a slight delamination in the clamping area caused during cutting, and thus, the results for this layup are not meaningful.

Young's Modulus $E = \mathbf{A}_E * f + \mathbf{C}_E$ @ $f = 50\ Hz \Rightarrow \boldsymbol{\eta}_{50}$				
Laminates	$\mathbf{A}_E$ x 10^{-4}	$\mathbf{C}_E$	$\boldsymbol{E}_{50}$	**H**
Flax (Non Hybrid)				
$[F_3^0]_s$	-2.0	25.37	25.36	100%
$[F_3^{90}]_s$	1.15	3.03	3.04	100%
$[F_3^{45}]_s$	4.53	5.88	5.99	100%
$[F^0/F^0/F^{90}]_s$	-2.1	21.77	21.76	100%
$[C^{90}/C^{90}/C^0]_s$	1.27	3.88	3.88	100%
$[FT_3^{0-90}]_s$	-0.18	13.62	13.62	100%
$[FT_3^{45}]_s$	4.66	6.44	6.46	100%
Carbon (Non Hybrid)				
$[C^0{}_3]_s$	-11.06	74.74	74.69	0%
$[C_3^{90}]_s$	21.82	6.16	6.16	0%
$[C_3^{45}]_s$	14.82	12.62	12.69	0%
$[C^0/C^0/C^{90}]_s$	-84.07	73.55	73.13	0%
$[C^{90}/C^{90}/C^0]_s$	9.53	6.33	6.38	0%
$[CT_3^{0-90}]_s$	-1.05	39.19	39.18	0%
$[CT_3^{45}]_s$	12.11	12.17	12.23	0%
Hybrid				
$[C^0/F^0/C^0]_s$	-4.53	57.7	57.67	33%
$[F^0/C^0/F^0]_s$	-0.56	32.80	32.79	66%
$[F^0/C^0/C^0]_s$	-3.16	32.73	32.73	33%
$[C^0/C^0/F^0]_s$	-2.09	68.79	68.78	33%
$[F^{90}/F^{90}/C^0]_s$	1.82	3.98	3.99	66%
$[C^0/F^{90}/F^{90}]_s$	-0.15	46.35	46.34	66%
$[C^0/F^{90}/C^0]_s$	-1.76	48.00	47.99	33%
$[F_2^{45}/C^0/F^{45}]_s$	-3.74	11.06	11.08	75%
$[C^0/F_3^{45}]_s$	-4.2	43.01	42.99	75%
$[F_2^{45}/C_2^0]_s$	4.53	5.88	5.90	50%

Table 5: Frequency-dependent Young's modulus models for investigated laminates

In Fig.10 the flax and carbon Young's moduli E_{50} for the different layups are compared. Here, a reversed relation of the values between damping and stiffness behavior is shown. As expected, carbon shows the significantly higher stiffness. In the fiber direction (UD0 and T0-90), the carbon laminate used is approximately three times as stiff as the flax laminate. Against the direction of the fibers (UD90) and with 45° laminates, the stiffness is still approximately twice as high.

For flax UD and twill, the Young's modulus known from the tensile tests [20] is met very accurately, validating the

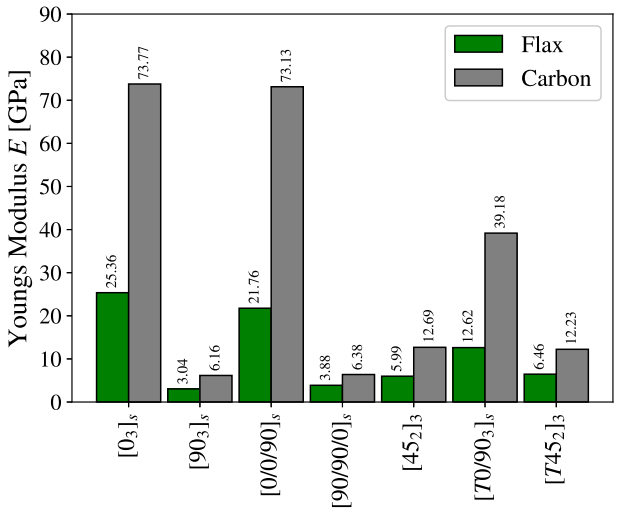

Fig. 10: Young's modulus E of flax vs. carbon with the same ply structure for $f = 50\ Hz$

used method. For UD0, the deviation is even less than 2%. However, the carbon stiffnesses from the data sheet are greatly undercut with a factor of 2.

Again, it shows, like expected for the stiffness that the outer layers dominate the behavior of the laminate. Thus, the inner plies have almost no influence on the stiffness as it can be seen for [0/0/90] and [90/90/0].

The results for the stiffness of the hybrids is shown in Fig. 11. Here, the hybrids are again arranged according to their degree of hybridization from left to right. It can be seen here too that it is not so much the degree of hybridization that influences the stiffness behavior, but rather the position of the plies, especially the UD0 plies. Comparing again $[C^0/C^0/F^0]_s$, $[C^0/F^0/C^0]_s$, and $[F^0/C^0/C^0]_s$, it is clear that the further the flax fiber is placed to the outside there is a concurrent reduction in stiffness. Flax layers in the inner layer results in a small reduction of stiffness of 7%. In the middle layers, E reduces by 30%, and in the outer layer about 50%.

4.3 Damping Stiffness Relation

For an application-related damping optimized design, the damping of the structure must always be set in relation to the stiffness. In aviation, the weight and thus the density also play a major role. The non-physical factor

$$E_s\eta = \frac{E * \eta}{\rho} \tag{5}$$

was therefore defined in order to relate the damping values to the stiffness. This is the loss factor η times Young's modulus E divided by the density ρ of the laminate. Even though this value cannot be a direct evaluation for use in a design because it sets the two material properties one-to-one, it can still evaluate the different materials in terms of

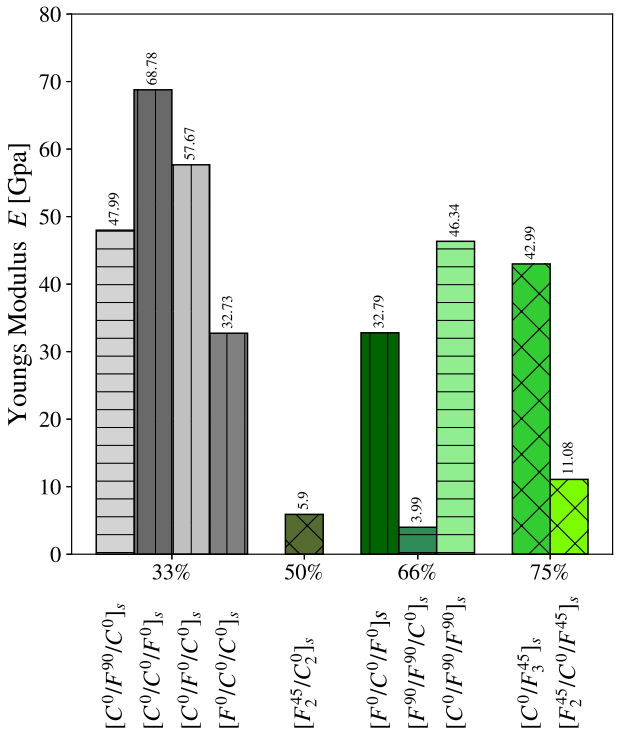

Fig. 11: Comparison of the Young's Modulus of hybrid laminates listed by degree of hybridization H (flax content in %) at $f = 50$ $f = 50$

their damping potential for comparison. The factor sets the different laminates in relation to each other:

$$F(E_s\eta) = \frac{E_s\eta_1}{E_s\eta_2} \tag{6}$$

In Fig.12 the factor F is plotted for all carbon and flax relations. In this case, $E_s\eta$ of the X-axis is $E_s\eta_1$ and $E_s\eta$ of the Y-axis is $E_s\eta_2$. The direct comparison between carbon and flax of the same layup is highlighted with red borders. It can be seen that flax performs significantly better for $E_s\eta$ with all laminates than carbon. Flax UD0 performs particularly well, offering a desirable combination of good stiffness and damping potential. $E_s\eta$ is 2.8 times better compared to UD0 carbon and better than any other laminate. For the others, the factor between flax and carbon is approximately two with the exception of $[90/90/0]_s$ and twill $[T0\text{-}90_3]_s$. The former has absolutely low values but a high difference factor between flax and carbon. When laid in the 0-90 direction as twill, flax performs in the relation factor $E_s\eta$ only slightly better than carbon. For carbon, the twill performs best.

Since the goal of this study is to hybridize carbon with flax to find a good compromise of damping and stiffness as a replacement for pure carbon components, the values η for the hybrids nominated on $E_s\eta$ of pure carbon in load direction (UD0) are particularly interesting. The percentage improvement of $E_s\eta$ by hybridization compared to pure carbon UD0 fibers is therefore shown in Fig13. Hybridization with UD0 flax fibers proves to be particularly effective.

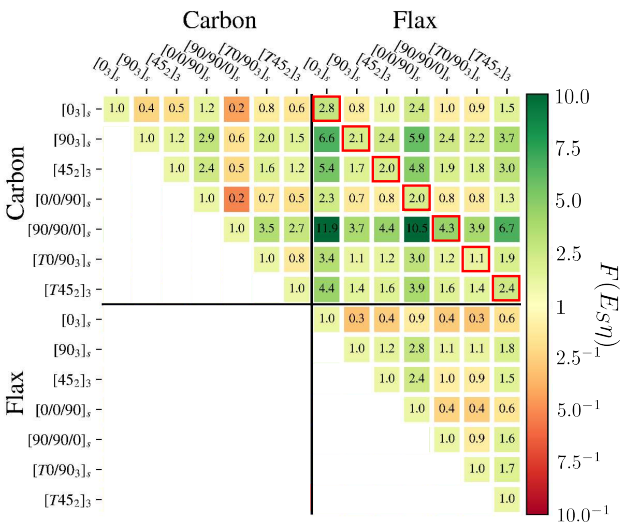

Fig. 12: Comparison of the relation factor $E_s\eta$ between different flax and carbon fiber orientations.

UD90, on the other hand, is less suitable, especially in hybridization, as it cannot develop the high damping potential due to the low stiffness. The same applies to 45 degree layers as an outer layer. Here, the percentage difference to flax is negative. As an inner layer, however, it could be an attractive solution.

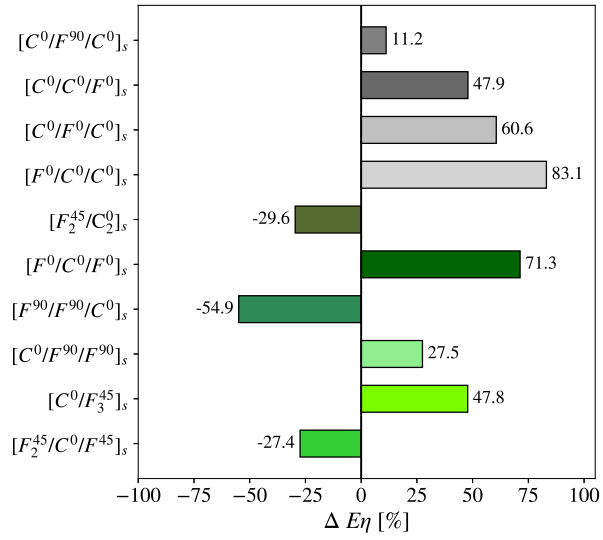

Fig. 13: Percentage improvement of $E_s\eta$ due to hybridization in relation to pure carbon UD0 laminate.

5. CONCLUSION

In this study, the damping behavior of flax, carbon and hybrid composites was tested and compared to their stiffness. For this purpose, frequency-dependent damping and stiffness models of the laminates were used with the aid of measurement results from experimental modal analysis. The damping behavior of flax and carbon could be quantified. The models can now be used in simulations and transferred to more complex structures. The damping properties were set in relation to the stiffness in order to be able to make an assessment for a potential improvement for application-related damping-optimized design .

The following conclusions could be drawn from the results:

1. The damping of the investigated flax fiber is significantly higher on laminate level than that of carbon fibers. The difference is particularly high for loads in the direction of the fibers. For the investigated fiber systems, flax dampens in UD0 up to seven times better.

2. The main influence on damping, as well as on stiffness, was shown to be the distance to the neutral axis of the plies. The dynamic behavior is almost exclusively determined by the outer layers, while the inner layers make almost no damping or stiffness contribution. Damping occurs mainly due to strain in the fibers.

3. Stiffness and damping were always opposed to each other. If one increases, the other decreases. By using flax fibers, however, it has been shown that it is possible to shift the damping/stiffness ratio in favor of damping by using the right ply structure.

4. The best results were achieved by hybridization with flax UD0, where the ratio between stiffness and damping gain is highest. This is where the damping of the fiber can have the greatest effect. 45° layers as inner layers can also be an attractive solution. The use of 90 degree ply flax yielded little benefit.

6. OUTLOOK

The laminates' damping showed a high dependency on the layup and the distance to the neutral axis of the flax fibers. Future investigations should go beyond laminate level and look at structural level damping. The load-bearing laminate has a significantly higher distance to the neutral axis in typical aerospace structures like double T-profiles or wing structures. It is expected that this will minimize the influence of the order of the plies. It also needs to be clarified whether other geometric effects are suitable for the targeted use of flax fibers to increase damping in structures.

In addition, the determined material values are now to be transferred to a damping model for simulations in order to be able to make better predictions for helicopter structures

7. ACKNOWLEDGMENT

This work is supported by the German Federal Ministry for Economic Affairs and Climate Action through the German Aviation Research Program LuFo VI-1 in the project

eVolve and InteReSt II. The author would like to thank Benedict Scheffler for contributing to this work during his term project.

Supported by:

Federal Ministry
for Economic Affairs
and Climate Action

on the basis of a decision
by the German Bundestag

8. COPYRIGHT STATEMENT

The authors confirm that they, and/or their company or organization, hold copyright on all of the original material included in this paper. The authors also confirm that they have obtained permission, from the copyright holder of any third party material included in this paper, to publish it as part of their paper. The authors confirm that they give permission, or have obtained permission from the copyright holder of this paper, for the publication and distribution of this paper as part of the ERF proceedings or as individual offprints from the proceedings and for inclusion in a freely accessible web-based repository.

REFERENCES

[1]Henschel, K. A., *Biocomposites in Aviation Structures on the Example of Flax and its Hybrids*, Ph.D. thesis, Technische Universität München, 2020.

[2]Datta, A., *Fundamental understanding, prediction and validation of rotor vibratory loads in steady-level flight*, University of Maryland, College Park, 2004.

[3]Kowarsch, U., Oehrle, C., and Keßler, M., editors, *High order CFD-simulation of the rotor fuselage interaction, 39th European Rotorcraft Forum*, 2013.

[4]Schaeferlein, U., Kessler, M., and Krämer, E., "Aeroelastic simulation of the tail shake phenomenon," *Journal of the American Helicopter Society*, Vol. 63, No. 3, 2018, pp. 1–17.

[5]Braun, "Development of antiresonance force isolators for helicopter vibration reduction," *Journal of the American Helicopter Society*, Vol. 27, No. 4, 1982, pp. 37–44.

[6]Rottmayr, H., Popp, W., and Mehlhose, R., "Application of modern vibration control techniques on EC135 and future trends," 1997.

[7]Rinker, M., Ries, T., Embacher, M., Platzer, S., Uhl, G., and Hajek, M., editors, *Simulation of Rotor–Empennage Interactional Aerodynamics in Comparison to Experimental Data*, 2019.

[8]Frederickson, K. C. and Lamb, editors, *Experimental investigation of main rotor wake induced empennage vibratory airloads for the RAH-66 Comanche helicopter*. American Helicopter Society, 1993.

[9]Leishman, G. J., *Principles of helicopter aerodynamics with CD extra*, Cambridge university press, 2006.

[10]Sheridan, P. F. and Smith, R. P., "Interactional aerodynamics—a new challenge to helicopter technology," *Journal of the American Helicopter Society*, Vol. 25, No. 1, 1980, pp. 3–21.

[11]Kus, A. e. a., editor, *An Advanced Five-Bladed Bearingless Main Rotor Dy-namics and Acoustics from Draft to Flight Test*, 2018.

[12]Yang, J., Xiong, J., Ma, L., Wang, B., Zhang, G., and Wu, L., "Vibration and damping characteristics of hybrid carbon fiber composite pyramidal truss sandwich panels with viscoelastic layers," *Composite Structures*, Vol. 106, 2013, pp. 570–580.

[13]Strohmann, K. and Hajek, M., editors, *An Eco-Efficient Helicopter Tailplane Hybridized from Flax, Balsa and Carbon*, 2019.

[14]Carus, M., Eder, A., Dammer, L., Korte, H., Scholz, L., Essel, R., Breitmayer, E., and Barth, M., "Wood-plastic composites (WPC) and natural fibre composites (NFC)," *Nova-Institute: Hürth, Germany*, Vol. 16, 2015, pp. 1–16.

[15]Ameur, B. M., El Mahi, A., Rebiere, J.-L., Abdennadher, M., and Haddar, M., "Damping Analysis of Unidirectional Carbon/Flax Fiber Hybrid Composites," *International Journal of Applied Mechanics*, Vol. Vol. 10, No. 05, 1850050, 2018.

[16]Duc, F., Bourban, P.-E., Plummer, C. J., and Månson, J.-A., "Damping of thermoset and thermoplastic flax fibre composites," *Composites Part A: Applied Science and Manufacturing*, Vol. 64, 2014, pp. 115–123.

[17]Fairlie, G. and Njuguna, J., "Damping properties of flax/carbon hybrid epoxy/fibre-reinforced composites for automotive semi-structural applications," *Fibers*, Vol. 8, No. 10, 2020, pp. 64.

[18]Assarar, M., Zouari, W., Sabhi, H., Ayad, R., and Berthelot, J.-M., "Evaluation of the damping of hybrid carbon–flax reinforced composites," *Composite Structures*, Vol. 132, 2015, pp. 148–154.

[19]Assarar, M., Zouari, W., Ayad, R., Kebir, H., and Berthelot, J.-M., "Improving the damping properties of carbon fibre reinforced composites by interleaving flax and viscoelastic layers," *Composites Part B: Engineering*, Vol. 152, 2018, pp. 248–255.

[20]Gaugelhofer, L., John, J., Yavrucuk, I., and Hajek, M., editors, *Experimental Investigation of Tensile Properties of Flax Fiber Reinforced Composites*, 2022.

[21]Duc, F., Bourban, P.-E., and Månson, J.-A. E., "Dynamic mechanical properties of epoxy/flax fibre composites," *Journal of Reinforced Plastics and Composites*, Vol. 33, No. 17, 2014, pp. 1625–1633.

[22]ASTM, "Standard Test Method for Measuring Vibration-Damping Properties of Materials," 2017.

[23]Pagani, A., Azzara, R., Carrera, E., and Zappino, E., "Static and dynamic testing of a full-composite VLA by using digital image correlation and output-only ground vibration testing," *Aerospace Science and Technology*, Vol. 112, 2021, pp. 106632.